Quantum Monte Carlo Study of the Two-Dimensional Homogeneous Electron Gas

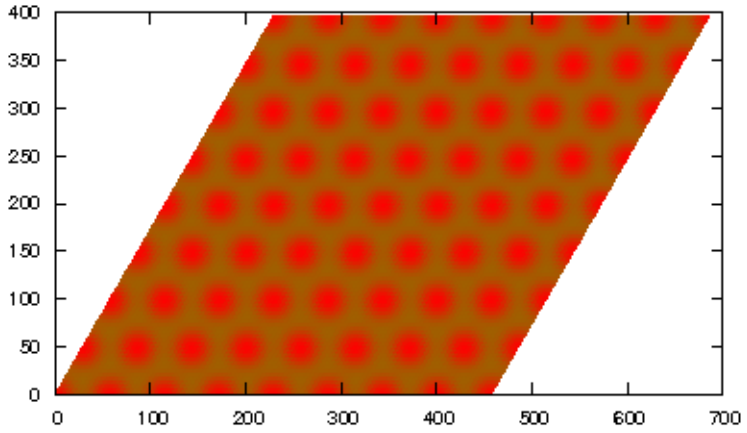

Neil D. Drummond

Department of Physics, Lancaster University

QMC and the CASINO program, TTI, Vallico Sotto, Italy

Wednesday 6th August, 2014

Two-Dimensional Homogeneous Electron Gas (I)

- 2D HEG: set of electrons moving in 2D in a uniform, inert, neutralising background.

- Hamiltonian (for finite system):

$$\hat{H} = \sum_i -\frac{1}{2}\nabla_i^2 + \sum_{j>i} v_E(\mathbf{r}_{ij}) + \frac{N v_M}{2}.$$

  Infinite-system ground-state energy per particle depends only on the **density** (specified by radius r_s of circle containing one electron on average) and **spin polarisation** [$\zeta = (N_\uparrow - N_\downarrow)/N$].

- Physical realisations:
  - *Electrons on metal surfaces.* E.g. Cu [111].
  - *Electrons on droplets of liquid He.*
  - *Inversion layers in MOS devices.* Can easily tune density. Electrons far from dopants; fewer complications due to disorder; technologically important.
  - Electrons in 2D semiconductors (gallium chalcogenides, etc.).

Two-Dimensional Homogeneous Electron Gas (II)

- **Quantum Monte Carlo** is the most accurate first-principles method available for studying the ground-state properties of the HEG.

- We have carried out QMC studies of the 2D HEG to determine:

  1. The zero-temperature phase diagram.[1]
  2. The pair-correlation function, structure factor and momentum distribution.[2]
  3. The energy band and hence quasiparticle effective mass.[3]

- Our data are of interest to

  – Experimentalists looking for ferromagnetism, Wigner crystallisation and changes to the effective mass in low-density 2D HEGs.
  – Theorists interested in constructing 2D XC functionals for DFT calculations.

[1] N. D. Drummond and R. J. Needs, Phys. Rev. Lett. **102**, 126402 (2009).
[2] N. D. Drummond and R. J. Needs, Phys. Rev. B **79**, 085414 (2009).
[3] N. D. Drummond and R. J. Needs, Phys. Rev. B **80**, 245104 (2009).

Wigner Crystallisation in 2D (I)

- Kinetic energy dominates at high density: *form Fermi fluid to minimise it.*
- Potential energy dominates at low density: *form Wigner crystal to minimise it.*
- Wigner crystals have been observed on the surface of liquid helium[4] and in inversion layers in MOSFET devices[5].
- Previous QMC studies[6] indicate that fluid–crystal transition occurs somewhere between $r_s = 25$ and 40 a.u. at zero temperature.
- Can we be more precise?

[4] C. C. Grimes and G. Adams, Phys. Rev. Lett. **42**, 795 (1979).
[5] E. Y. Andrei *et al.*, Phys. Rev. Lett. **60**, 2765 (1988); R. L. Willett *et al.*, Phys. Rev. B **38**, 7881 (1988).
[6] B. Tanatar & D. M. Ceperley, Phys. Rev. B **39**, 5005 (1989); F. Rapisarda & G. Senatore, Aust. J. Phys. **49**, 161 (1996).

Wigner Crystallisation in 2D (II)

- Triangular lattice has lowest Madelung constant. Wins at low density.
- Hartree–Fock theory[7]: antiferromagnetic square lattice $\rightarrow$ ferromagnetic triangular lattice at $r_s = 2.6$ a.u.
- We consider only triangular lattices.

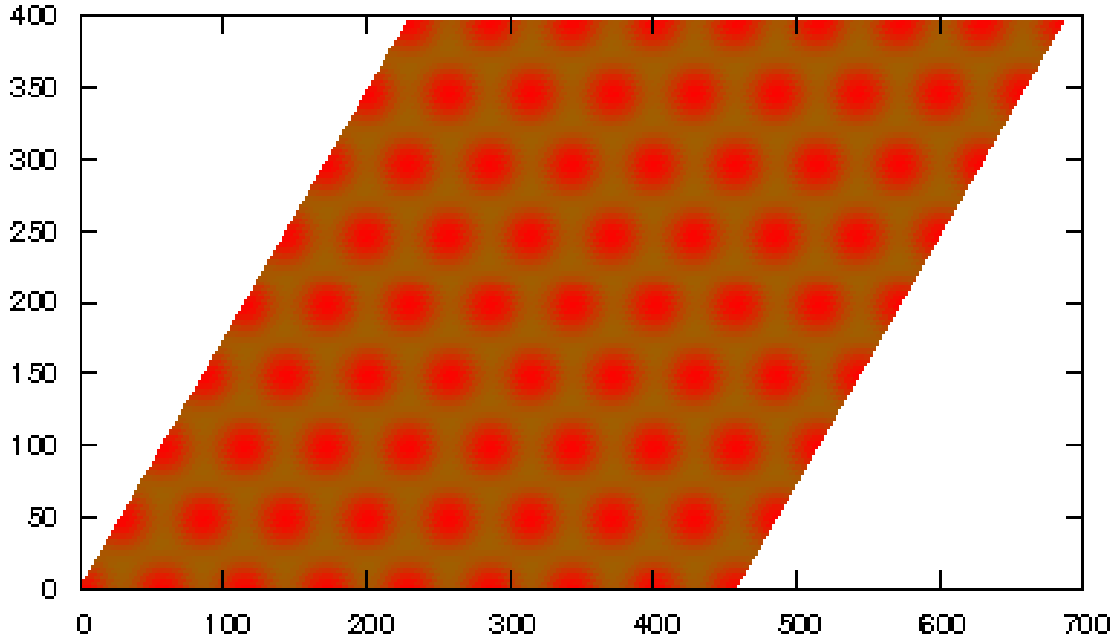

[7] J. R. Trail, M. D. Towler and R. J. Needs, Phys. Rev. B **68**, 045107 (2003).

Magnetic Behaviour of the Fermi Fluid (I)

- Bloch transition: paramagnetic fluid favoured at high density (doubly occupy low-momentum states to minimise KE); ferromagnetic fluid favoured at low density (keep electrons apart to minimise XC energy).

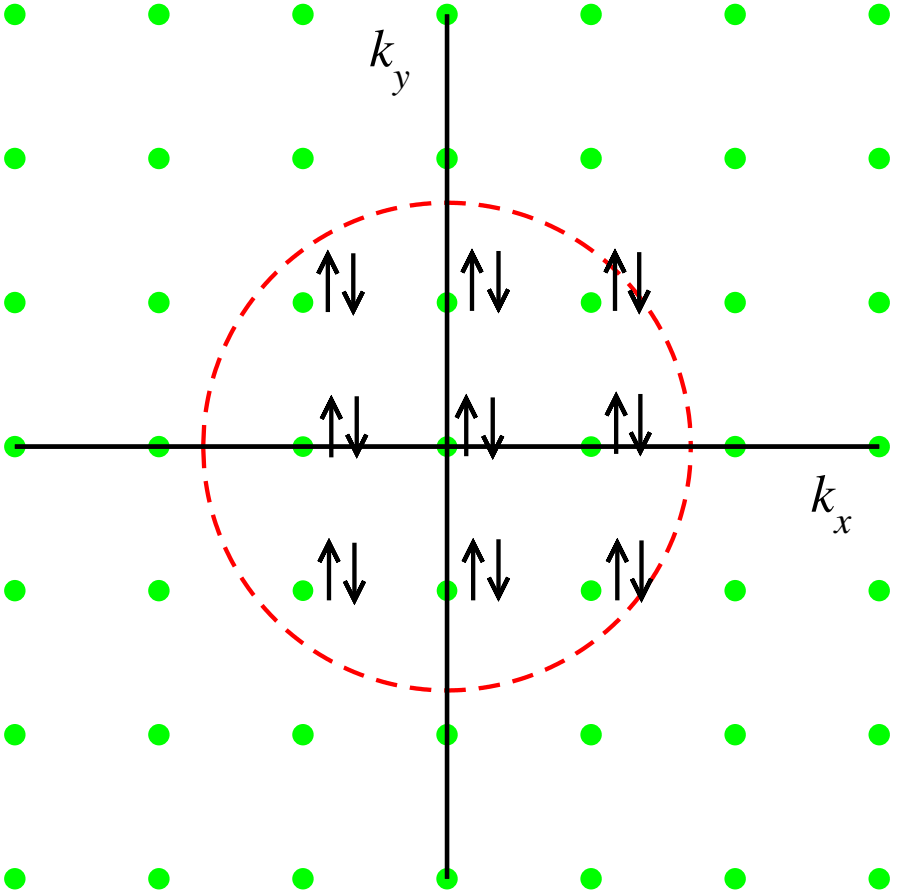

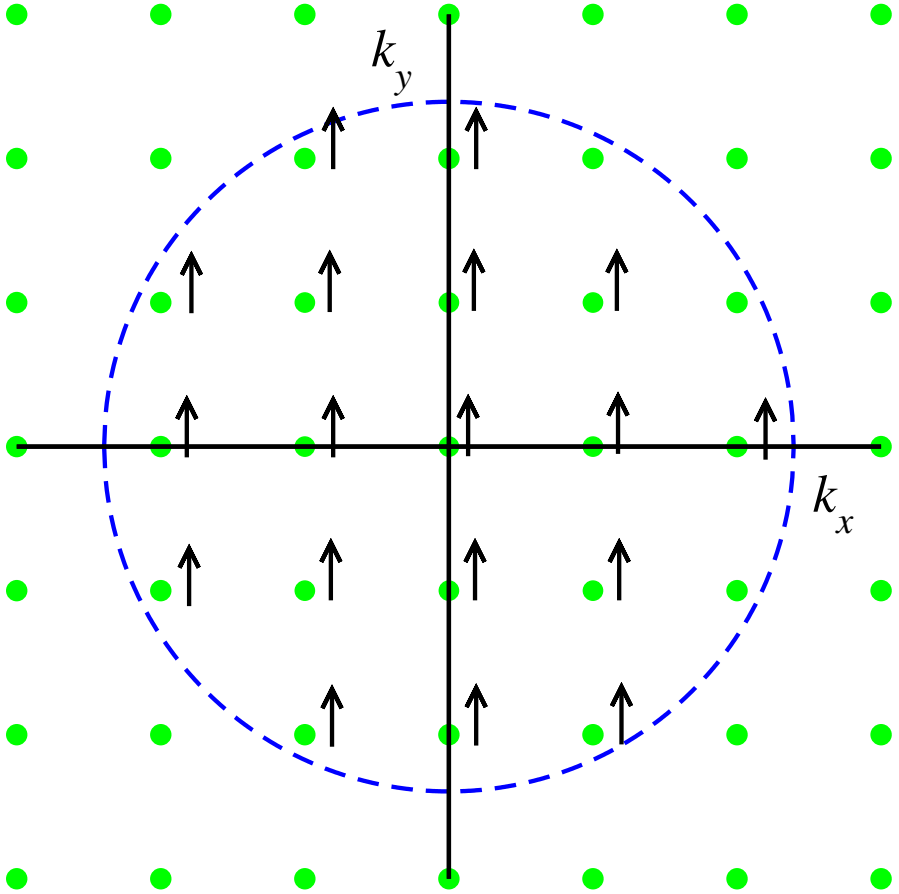

Magnetic Behaviour of the Fermi Fluid (II)

- Hartree–Fock theory: Bloch transition at $r_s = 2.01$ a.u. No region of stability for ferromagnetic fluid.
- VMC[8]: Bloch transition at $r_s = 13(2)$ a.u.; crystallisation at $r_s = 33(2)$ a.u.
- DMC[9]: Bloch and crystallisation transitions at $r_s = 37(5)$ a.u.
- DMC[10]: Bloch transition at $r_s = 20(2)$ a.u. and crystallisation at $r_s = 34(4)$ a.u.
- Experiment[11]: "Possible evidence" of spontaneous spin polarisation at $r_s = 7.6$ a.u.
- Open question: is there a range of densities at which the 2D HEG forms a ferromagnetic fluid?

---

[8] D. Ceperley, Phys. Rev. B **18**, 3126 (1978).
[9] B. Tanatar and D. M. Ceperley, Phys. Rev. B **39**, 5005 (1989).
[10] F. Rapisarda and G. Senatore, Aust. J. Phys. **49**, 161 (1996).
[11] A. Ghosh, C. J. B. Ford, M. Pepper, H. E. Beere and D. A. Ritchie, Phys. Rev. Lett. **92**, 116601 (2004).

Magnetic Behaviour of the Wigner Crystal

- Hartree-Fock theory[12]: ferromagnetic for $r_s > 2.6$ a.u.
- Multispin exchange model[13]: frustrated antiferromagnetism (spin liquid) $\rightarrow$ ferromagnetism at $r_s \leq 175(10)$ a.u.
- We have studied both ferromagnetic and antiferromagnetic triangular crystals.
- We have used striped antiferromagnetic crystals. Energy should be close to that of the spin liquid.

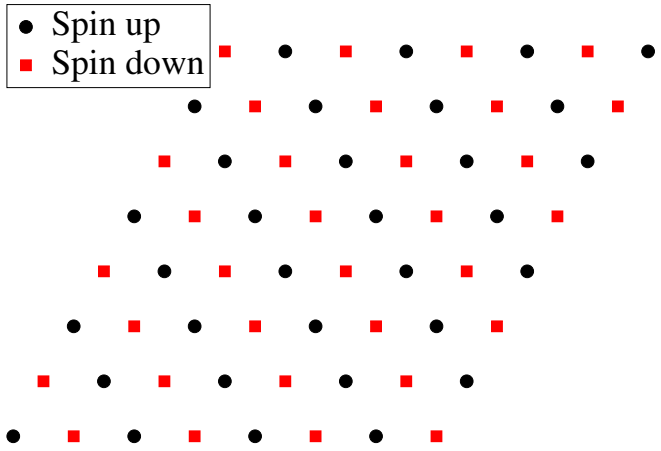

[12] J. R. Trail, M. D. Towler and R. J. Needs, Phys. Rev. B **68**, 045107 (2003).
[13] B. Bernu, L. Candido and D. M. Ceperley, Phys. Rev. Lett. **86**, 873 (2001).

Fermi Fluid: Boundary Conditions (I)

- Orbitals for Fermi fluid:

$$\phi_{\mathbf{k}}(\mathbf{r}) = \exp(i\mathbf{k}\cdot\mathbf{r}).$$

- Periodic boundary conditions on a finite cell: $\{\mathbf{k}\}$ are simulation-cell $\mathbf{G}$-vectors.

- *Single-particle finite-size effects:* Increase N at fixed density; grid of $\mathbf{G}$-vectors gets finer; energy per electron jumps as shells of $\mathbf{G}$ vectors get occupied.

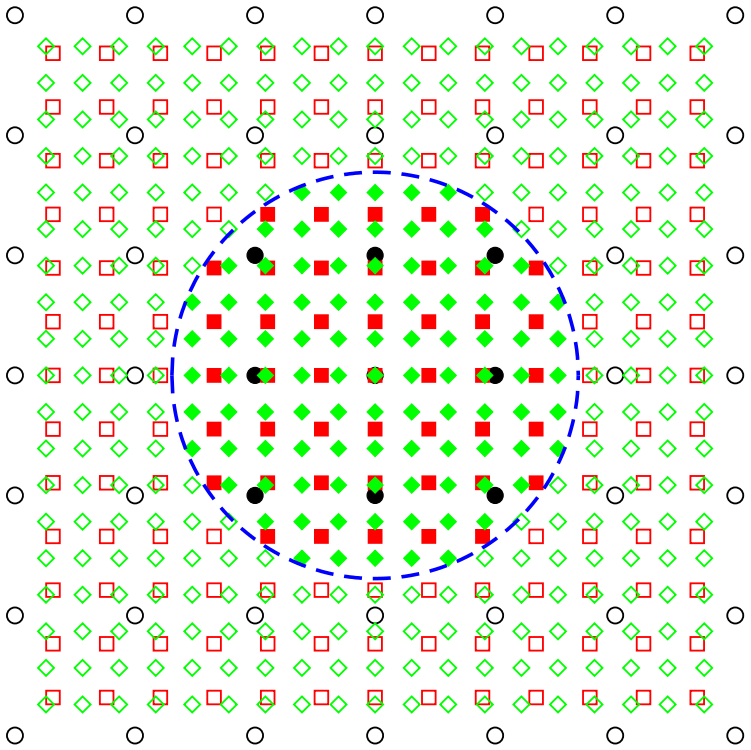

Fermi Fluid: Boundary Conditions (II)

- Twisted boundary conditions: $\mathbf{k}$ are simulation-cell $\mathbf{G}$ vectors offset by $\mathbf{k}_s \in$ 1st Brillouin zone of simulation cell.

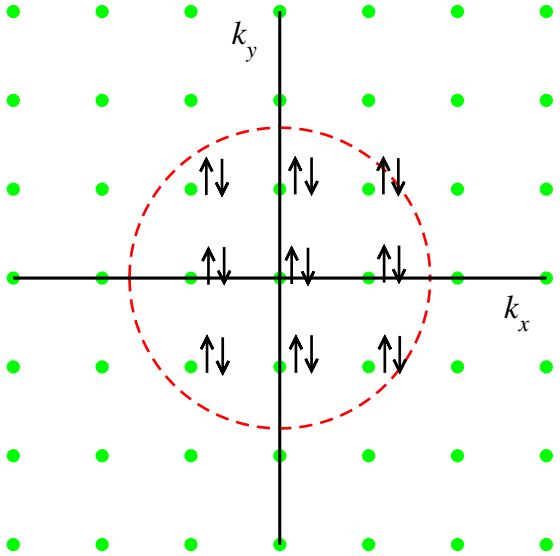

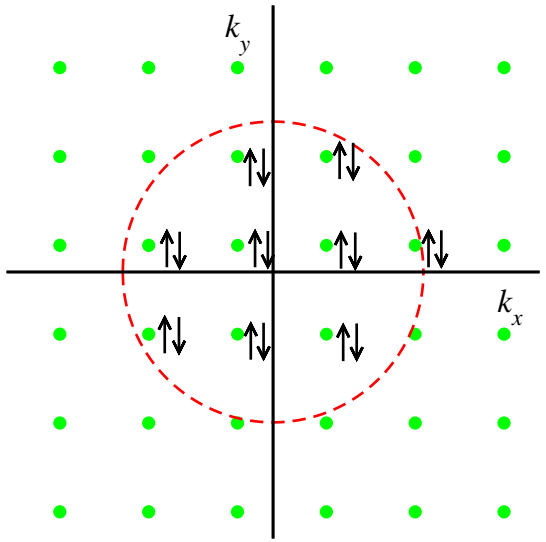

- Twist averaging in canonical ensemble: average over all $\mathbf{k}_s$, keeping N fixed.
  - Replaces grid of $\mathbf{k}$ by a Fermi area (equal to area of Fermi circle), greatly reducing single-particle finite-size effects.
  - Shape isn't quite right: leaves small positive bias in KE.

- Previous QMC studies of 2D HEG have not used twist averaging.

Long-Range Finite-Size Errors

- Compression of XC hole and neglect of long-range two-body correlations in finite cell give error in 2D energy per electron going as $\mathcal{O}(N^{-5/4})$.[14] Extrapolate using:

$$E_N = E_\infty - bN^{-5/4}.$$

- Previous QMC studies have used $N^{-3/2}$ for crystals and N^{-1} for fluid.

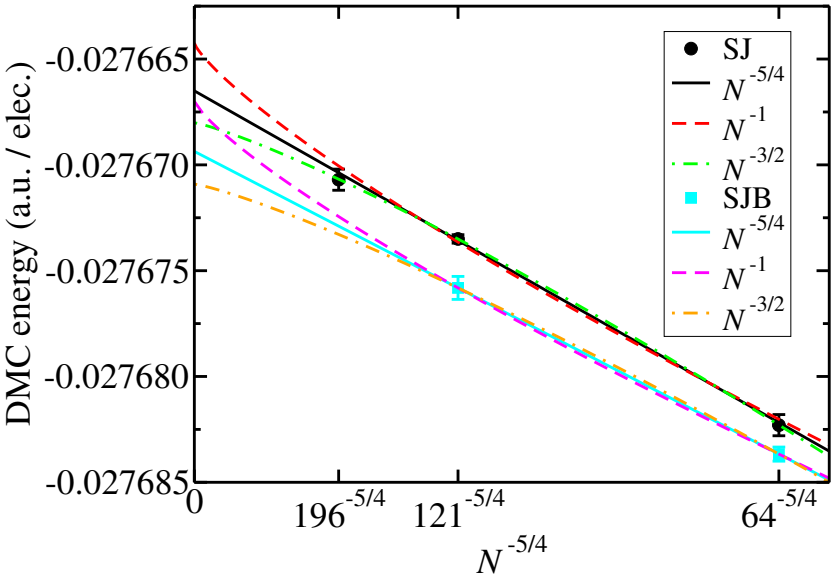

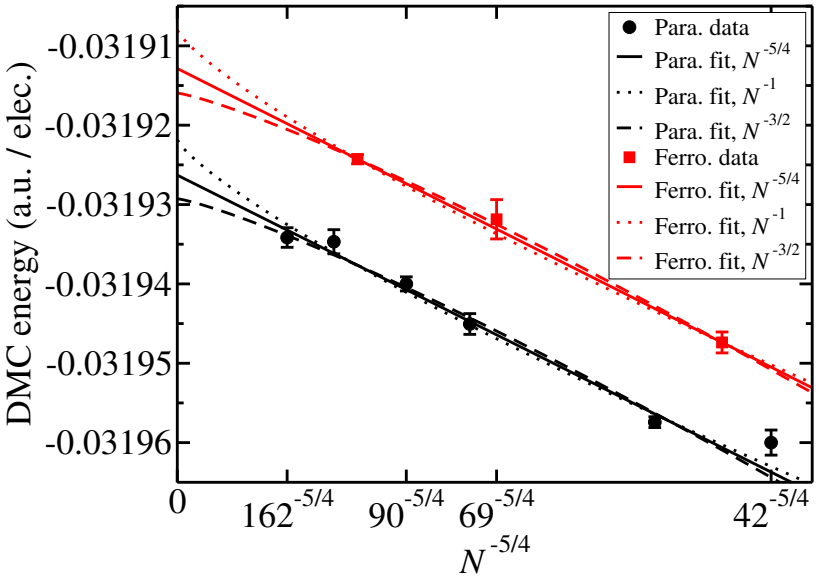

Left: crystal extrapolation at $r_s = 35$ a.u.; right: fluid extrapolation at $r_s = 30$ a.u.

[14] N. D. Drummond, R. J. Needs, A. Sorouri and W. M. C. Foulkes, Phys. Rev. B **78**, 125106 (2008).

Backflow Transformation

- Evaluate Slater wave function at quasiparticle coordinates related to actual electron coordinates by electron–electron **backflow** functions.[15]

- Moves nodal surface of wave function; can improve the fixed-node DMC energy.

- BF is more significant in fluids than crystals, where electrons are already kept apart by localisation on lattice sites.

- Parallel spins are already kept away from each other by wave-function antisymmetry. BF is much less important in ferromagnetic systems.

System ($r_s = 30$ a.u.)	Lowering of DMC energy due to BF (μHa / elec.)
Paramagnetic fluid	$36(3)$
Ferromagnetic fluid	$6(4)$
Antiferromagnetic crystal	$2.4(6)$
Ferromagnetic crystal	$2.3(3)$

[15] P. López Ríos, A. Ma, N. D. Drummond, M. D. Towler and R. J. Needs, Phys. Rev. E **74**, 066701 (2006).

Optimisation of Crystal Orbitals (I)

- Crystal orbitals: $\phi_{\mathbf{R}}(\mathbf{r}) = \exp(-C|\mathbf{r} - \mathbf{R}|^2)$.

- Only orbital parameter affecting crystal nodal surface: Gaussian exponent C.
  - Minimise DMC energy w.r.t. C to minimise fixed-node error.
  - Then add backflow.

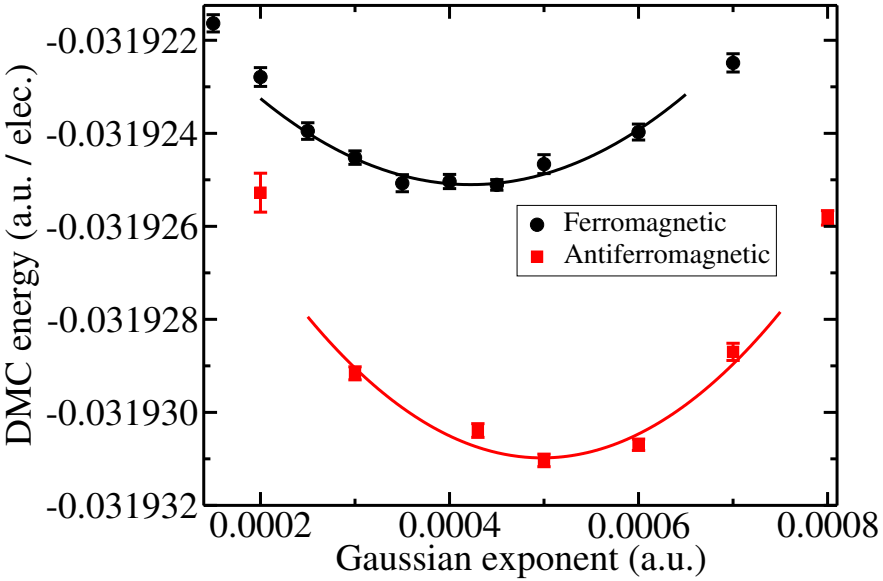

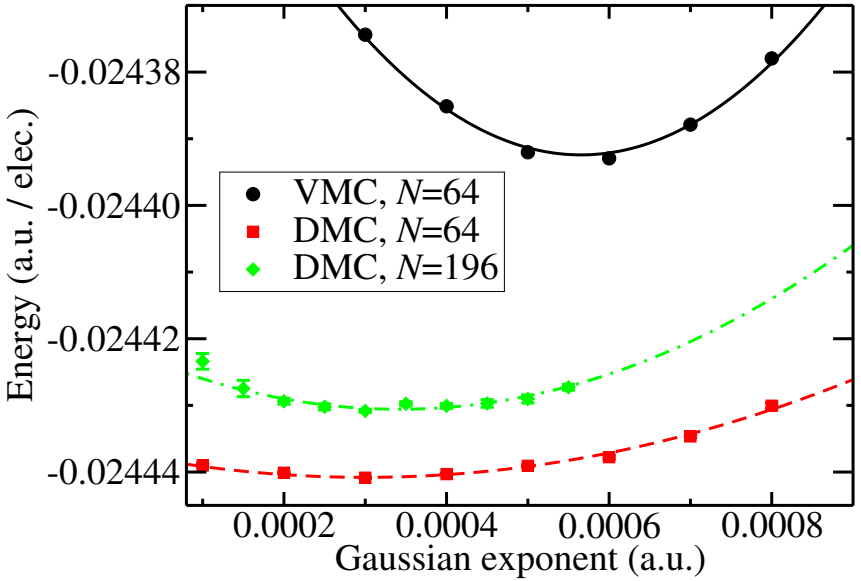

DMC energy against C at $r_s = 30$ a.u. (left) and $r_s = 40$ a.u. (right) (ferro.).

Optimisation of Crystal Orbitals (II)

- Ferromagnetic crystals: optimal exponent is $C^{\mathrm{F}}_{\mathrm{DMC}} = 0.071 r_s^{-3/2}$.
  - CF, VMC exponent is $C^{\mathrm{F}}_{\mathrm{VMC}} = 0.15 r_s^{-3/2}$;
  - HF exponent is $C^{\mathrm{F}}_{\mathrm{HF}} = 0.46 r_s^{-3/2}$.

- Antiferromagnetic crystals: optimal exponent is $C^{\mathrm{AF}}_{\mathrm{DMC}} = 0.082 r_s^{-3/2}$.

2D HEG Energy Diagram (I)

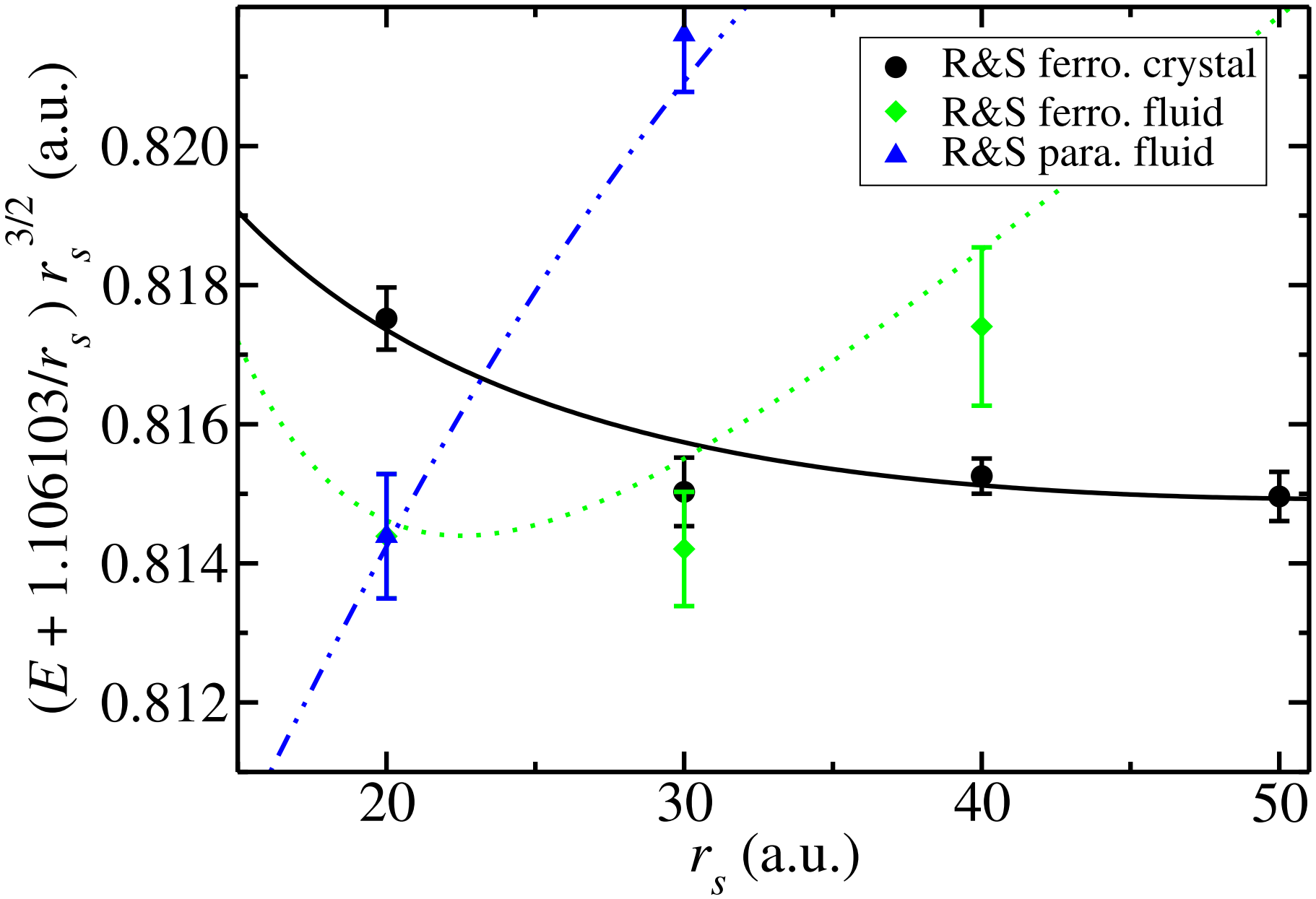

2D HEG Energy Diagram (I)

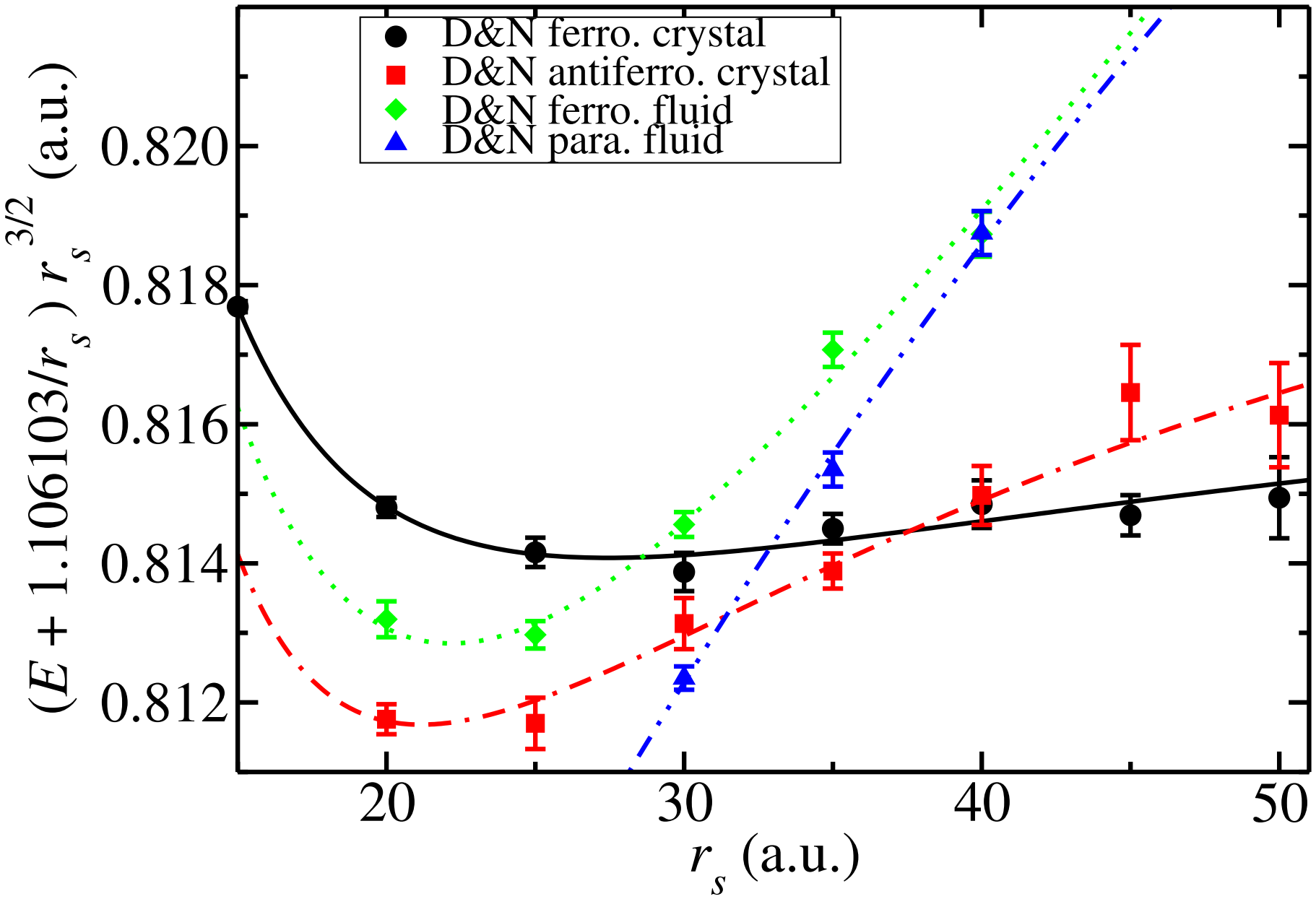

2D HEG Energy Diagram (II)

- Fully polarised fluid is never stable.
- Wigner crystallisation occurs at $r_s = 31(1)$ a.u. Transition is from a **paramagnetic fluid** to an **antiferromagnetic Wigner crystal**.
- Further transition: **antiferromagnetic** $\rightarrow$ **ferromagnetic** crystal at $r_s = 38(5)$ a.u.
- At $r_s = 35$ a.u., the energy of a fluid with $\zeta = 2/5$ agrees with the paramagnetic and ferromagnetic fluid energies.
  - Very unlikely that a region of stability for a partially polarised fluid exists.
- Phase transitions in 2D HEG cannot be first order.[16]
  - It's energetically favourable to form boundaries between macroscopically separated phases, so a "microemulsion" is formed at crystallisation density.
  - New phases could "round off corners" in energy diagram.

[16] B. Spivak and S. A. Kivelson, Phys. Rev. B **70**, 155114 (2004); R. Jamei *et al.*, Phys. Rev. Lett. **94**, 056805 (2005).

Contact PCF of Paramagnetic Fluid (I)

- $g(0)$ is an important parameter in construction of GGA XC functionals for use in DFT.

- Most theoretical calculations of $g(0)$ have used *ladder theory* to solve approximately the Bethe–Goldstone equation for the effective interaction between two electrons. Exact in high-density limit, but not at low densities.

- Disagreement between old approximation[17] in ladder theory and a better approximation,[18] and between the better approximation in ladder theory and QMC.[19] *Which is right?*

- We evaluate $g(r)$ [including $g(0)$] by binning interparticle distances. Easier in 2D than 3D. Easier at high density than low density.

- Earlier study used Slater–Jastrow wave function and no twist averaging; ours used Slater–Jastrow–backflow wave functions and twist averaging.

[17] S. Nagano, K. S. Singwi, and S. Ohnishi, Phys. Rev. B **29**, 1209 (1984); *Erratum*, Phys. Rev. B **31**, 3166 (1985).
[18] Z. Qian, Phys. Rev. B **73**, 035106 (2006).
[19] P. Gori-Giorgi, S. Moroni, and G. B. Bachelet, Phys. Rev. B **70**, 115102 (2004).

Contact PCF of Paramagnetic Fluid (II)

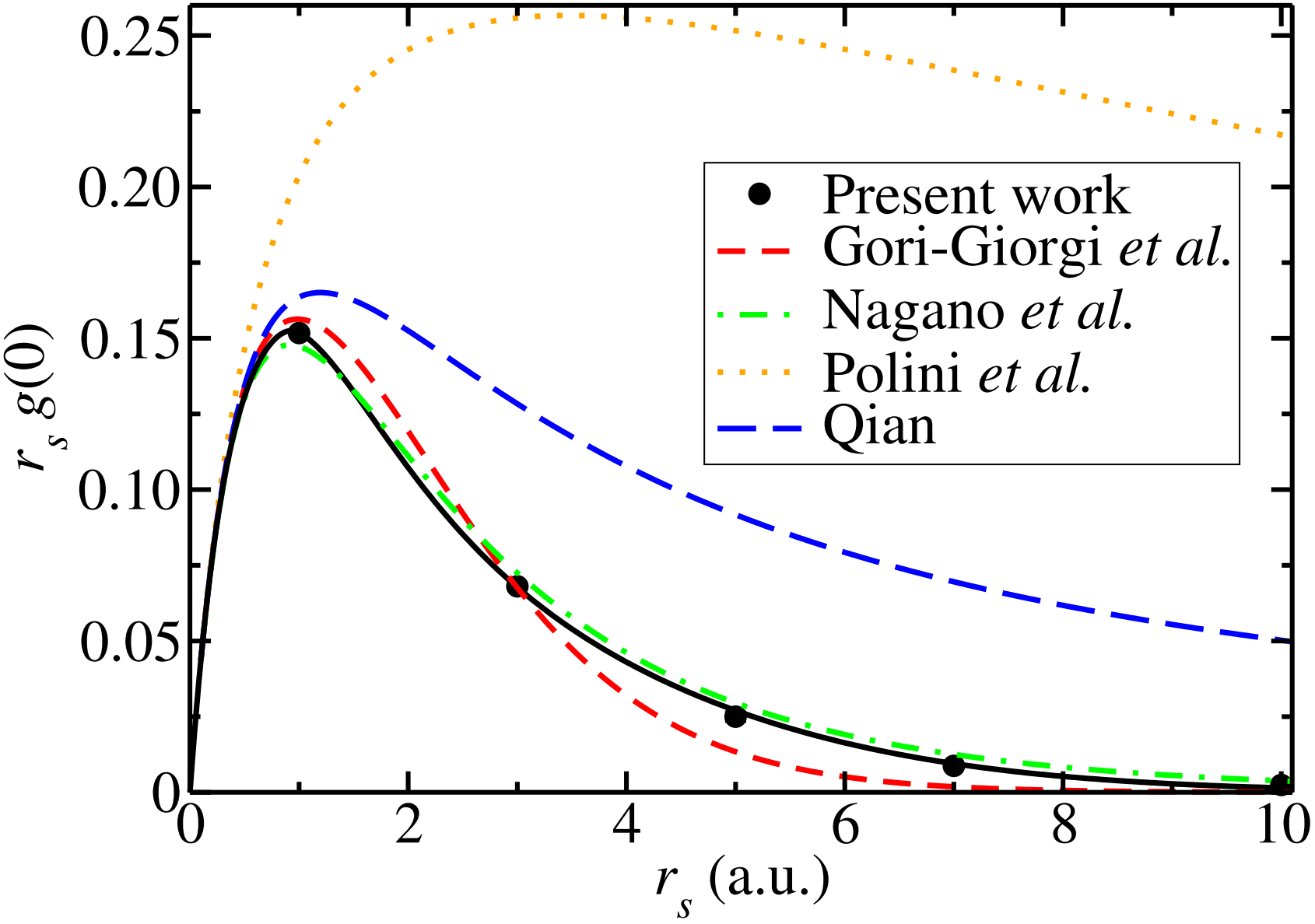

Fermi Liquid Theory

- Fermi liquid theory[20]: *low-energy excitations in a fluid of interacting electrons can be treated as excitations of* quasiparticles *occupying plane-wave states.*

- Justification: Pauli exclusion principle. Scattering rate of quasiparticles between plane waves is low (vanishes at Fermi surface). Single-particle momenta are approximately good quantum numbers.

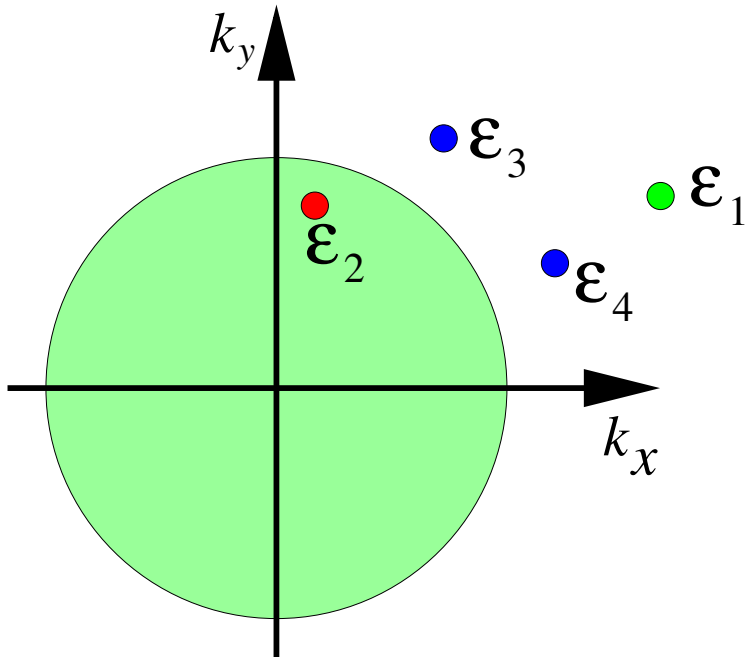

[20] L. D. Landau, JETP **3**, 920 (1957); L. D. Landau, JETP **5**, 101 (1957); L. D. Landau, JETP **8**, 70 (1959).

Landau Energy Functional

- Total energy E:

$$E = E_0 + \sum_{\mathbf{k},\sigma} \mathcal{E}_\sigma(\mathbf{k}) \delta N_{\mathbf{k},\sigma} + \frac{1}{2} \sum_{\mathbf{k},\sigma} \sum_{\mathbf{k}',\sigma'} f_{\sigma\sigma'}(\mathbf{k},\mathbf{k}') \delta N_{\mathbf{k},\sigma} \delta N_{\mathbf{k}',\sigma'},$$

  where E_0 is the ground-state energy and $\delta N_{\mathbf{k},\sigma}$ is the change in quasiparticle occupancy relative to the ground state.

- Quasiparticle energy band: $\mathcal{E}_\sigma(\mathbf{k})$ is the energy of an isolated quasiparticle.
  - Linear approximation: near the Fermi surface, $\mathcal{E}_\sigma(\mathbf{k}) = \mathcal{E}_F + (k_F/m^*)(k - k_F)$, where $\mathcal{E}_F$ is the Fermi energy and m^* is the quasiparticle effective mass.

- Landau interaction function: $f_{\sigma\sigma'}(\mathbf{k},\mathbf{k}')$ describes quasiparticle interactions.
  - Near the Fermi surface, $f_{\sigma\sigma'}$ only depends on the angle $\theta_{\mathbf{k}\mathbf{k}'}$ between $\mathbf{k}$ and $\mathbf{k}'$.

Quasiparticle Effective Mass of the 2D HEG

- The effective mass (m^*) of a paramagnetic 2D HEG has been the subject of great controversy in recent years:
  - Some experiments[21] found a large enhancement of m^* at low density; other experiments[22] have contradicted this.
  - GW calculations give a range of possible results depending on the choice of effective interaction.[23]
  - Previous QMC studies have predicted (i) much less[24] and (ii) much more[25] enhancement of m^* than found in recent experiments.

- Experiment[22] and theory[26] suggest that m^* in paramagnetic and ferromagnetic HEGs behaves quite differently as a function of density.

---

[21] J. L. Smith and P. J. Stiles, Phys. Rev. Lett. **29**, 102 (1972); V. M. Pudalov *et al.*, Phys. Rev. Lett. **88**, 196404 (2002).
[22] Y.-W. Tan *et al.*, Phys. Rev. Lett. **94**, 016405 (2005); M. Padmanabhan *et al.*, Phys. Rev. Lett. **101**, 026402 (2008).
[23] G. F. Giuliani and G. Vignale, *Quantum Theory of the Electron Liquid*, CUP, Cambridge (2005).
[24] Y. Kwon, D. M. Ceperley, and R. M. Martin, Phys. Rev. B **50**, 1684 (1994).
[25] M. Holzmann, B. Bernu, V. Olevano and D. M. Ceperley, Phys. Rev. B **79**, 041308(R) (2009).
[26] Y. Zhang and S. Das Sarma, Phys. Rev. Lett. **95**, 256603 (2005).

Calculating the Effective Mass and Landau Interaction Functions

- To calculate the quasiparticle effective mass:
  - The DMC energy band $\mathcal{E}(k)$ was determined at a range of k by taking the energy difference when an electron is added to or removed from a closed-shell ground-state.
  - A quartic $\mathcal{E}(k) = \alpha_0 + \alpha_2 k^2 + \alpha_4 k^4$ was fitted to the energy band values.
  - The effective mass was then calculated as $m^* = k_F/(d\mathcal{E}/dk)_{k_F}$.

- To calculate the Landau interaction functions and hence Fermi liquid parameters:
  - Electrons were promoted from $(\sigma, \mathbf{k})$ just below the Fermi edge to $(\sigma', \mathbf{k}')$ just above it, to obtain the energy difference $\Delta E_{\sigma\sigma'}(\mathbf{k}, \mathbf{k}')$ relative to the ground state.
  - The single-particle contribution was subtracted from the excitation energy, to give $-f_{\sigma\sigma'}(\theta_{\mathbf{k}\mathbf{k}'}) = \Delta E_{\sigma\sigma'}(\mathbf{k}, \mathbf{k}') - [\mathcal{E}(\mathbf{k}') - \mathcal{E}(\mathbf{k})]$.
  - The first few Fourier components of $f_{\sigma\sigma'}(\theta)$ were found by numerical integration in order to obtain the *Fermi liquid parameters*.

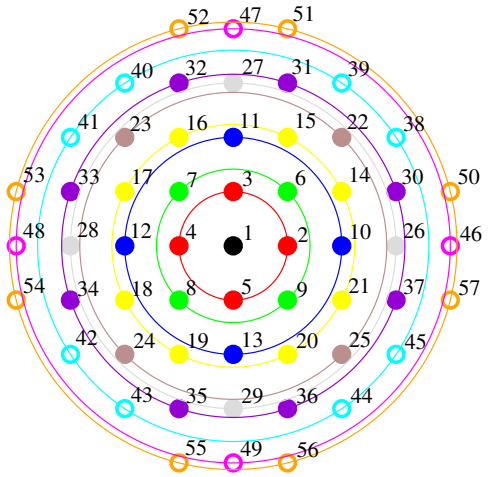

Fermi Liquid Parameters

- Fermi liquid parameters:

$$F_l^{s,a} = \frac{Am^*}{4\pi^2} \int \left[f_{\uparrow\uparrow}(\theta_{\mathbf{kk}'}) \pm f_{\uparrow\downarrow}(\theta_{\mathbf{kk}'}) \right] \cos(l\theta)\, d\theta,$$

  where $A = \pi r_s^2 N$ is the area of the simulation cell.

- For a ferromagnetic HEG, the Fermi liquid parameters $\{F_l\}$ are given by the expression above with $f_{\uparrow\downarrow} = 0$.

- *We need to obtain a description of the interaction parameters according to a well-defined prescription for energy differences in a finite cell, then extrapolate the Fermi liquid parameters to the thermodynamic limit.*

- Armed with the effective mass and the Fermi liquid parameters, nearly all thermodynamic and transport properties of the fully interacting electron gas can be calculated.

Finite-Size Errors

- The calculations were performed in finite cells subject to periodic boundary conditions.
- Major source of error and uncertainty in the QMC results: finite size effects.
- Momentum quantisation:
  - In our finite simulation cell subject to (twisted) periodic boundary conditions, the available momentum states fall on the (offset) grid of reciprocal lattice points.
  - This restricts the $\mathbf{k}$ values we can consider.

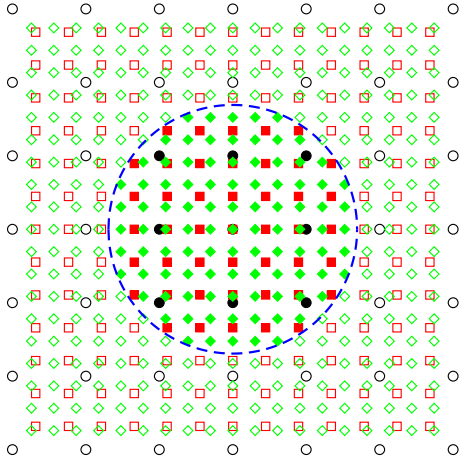

- There are also finite size errors in the excitation energies due to the neglect of long-range interactions and correlations in a finite cell.
  - These errors have been shown to fall off slowly, as $N^{-1/4}$, near the Fermi surface.[27]

[27] M. Holzmann, B. Bernu, V. Olevano and D. M. Ceperley, Phys. Rev. B **79**, 041308(R) (2009).

Pathological Behaviour at the Fermi Surface (I)

- Fermi liquid theory is only valid near the Fermi surface.
- Energy band is defined by Landau energy functional at all $\mathbf{k}$, but does not correspond to quasiparticle band except near Fermi surface.
- In the infinite-system limit, the exact energy band is smooth and well-behaved everywhere, including the Fermi surface.
- The Hartree–Fock band is pathological.
  - In the infinite-system limit it has a logarithmic divergence at the Fermi surface.
  - In finite systems it behaves very badly.

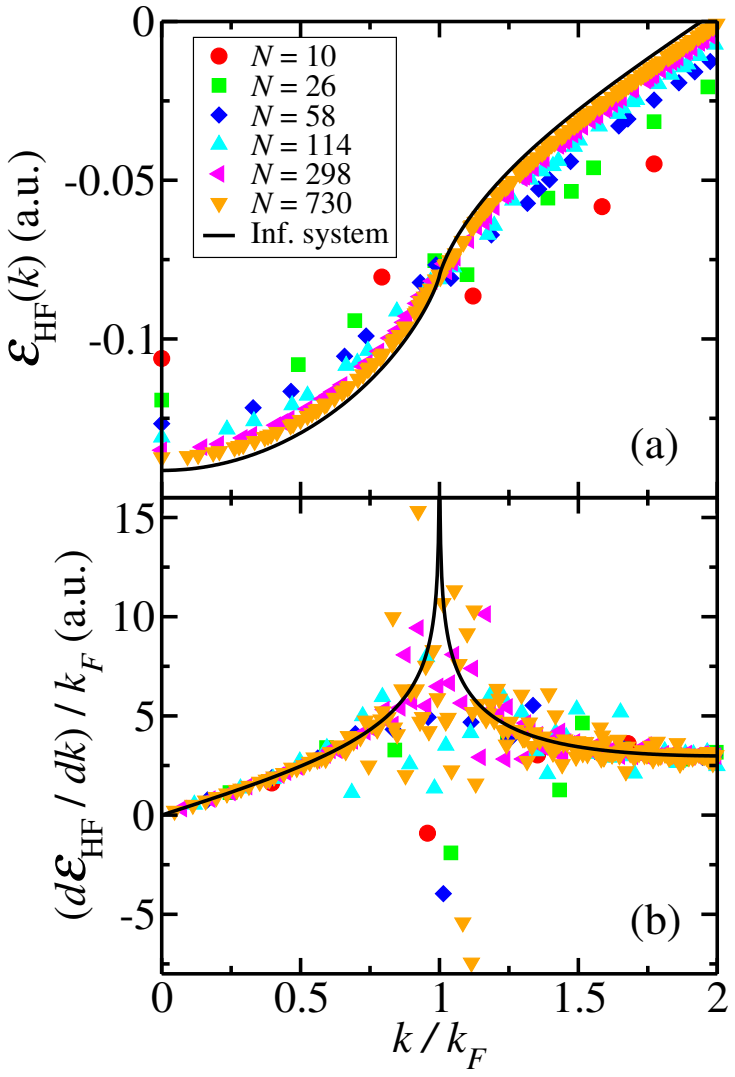

Pathological Behaviour at the Fermi Surface (II)

- *DMC may take you 99% of the way from HF to reality, but this does not get rid of the pathological behaviour from HF theory.*

- Hence we need to consider excitations **away from the Fermi surface** in order to obtain the gradient of the energy band at k_F.

- Finite-size effects in the Fermi liquid parameters are a killer.

Assessing the Accuracy of our DMC Calculations (I)

- Occupied bandwidth: $\Delta\mathcal{E} = \mathcal{E}(k_F) - \mathcal{E}(0) = E_-(0) - E_-(k_F)$.

- DMC BW is expected to be an upper bound: assuming DMC retrieves the same fraction of the correlation energy in the ground and excited states, the BW will lie between the Hartree-Fock value $E_-^{\rm HF}(0) - E_-^{\rm HF}(k_F)$, which is too large, and the exact result $E_-^{\rm exact}(0) - E_-^{\rm exact}(k_F)$.

- Likewise, Slater-Jastrow DMC BWs are expected to be greater than Slater-Jastrow-backflow DMC BWs.

- *To obtain an accurate BW, it is essential to retrieve a very large fraction of the correlation energy in the DMC calculations, which explains why the inclusion of backflow is so important.*

- The extent to which the BW is overestimated in HF theory grows with r_s so that, assuming DMC retrieves a constant fraction of the correlation energy, the DMC bands become less accurate at low density.

Assessing the Accuracy of our DMC Calculations (II)

- Extrapolating the VMC energy with different trial wave functions to zero variance suggests that our DMC calculations retrieve more than 99% of the correlation energy, and that the fraction retrieved is similar in both the ground and excited states.

- The free-electron BW is greater than or approximately equal to the exact BW. Hence the error in the HF BW is less than or approximately equal to $\Delta\mathcal{E}^{\mathrm{HF}} - \Delta\mathcal{E}^{\mathrm{free}} = k_F(1-2/\pi)$.

- So the error in the DMC BW is less than $0.01k_F(1-2/\pi) \approx 0.007/r_s$ for a ferromagnetic HEG and less than about $0.01k_F(1-2/\pi) \approx 0.005/r_s$ for a paramagnetic HEG.
  - Since the BW falls off as r_s^{-2}, the error is more significant at large r_s.
  - In the worst case (the paramagnetic HEG at $r_s = 10$) this argument suggests that DMC overestimates the BW by $\sim 9\%$. In the next-worse case (paramagnetic, $r_s = 5$), the BW is overestimated by $\sim 4\%$.
  - It is reasonable to assume that DMC underestimates m^* by a similar amount.

To Reoptimise or Not To Reoptimise

- We optimise the trial wave function in the ground state and then continue to use the same Jastrow factor and backflow function in our excited-state calculations.

- The excitation of a single electron has no effect on the optimal Jastrow factor or backflow function in the thermodynamic limit.
  - Hence the fact that the Jastrow factor and backflow function can be re-optimised in an excited state in a finite cell[28] is simply a finite-size effect.
  - More finite-size bias is introduced into the energy band by re-optimising the Jastrow factor and backflow function in each excited state considered.

- It is essential not to re-optimise the wave function when an electron is promoted, to maximise the cancellation of errors that occurs when the single-particle contribution is subtracted out from a difference in total energy.

- Promoting an electron results in smaller finite-size errors than adding two electrons, since the latter modifies the density of the finite system.

[28] For example, re-optimising the wave function when an electron is subtracted from $\mathbf{k} = \mathbf{0}$ in a 74-electron HEG at $r_s = 1$ lowers the DMC energy by $0.000241(4)$ a.u.

Paramagnetic Single-Particle Energy Band: $r_s = 1$

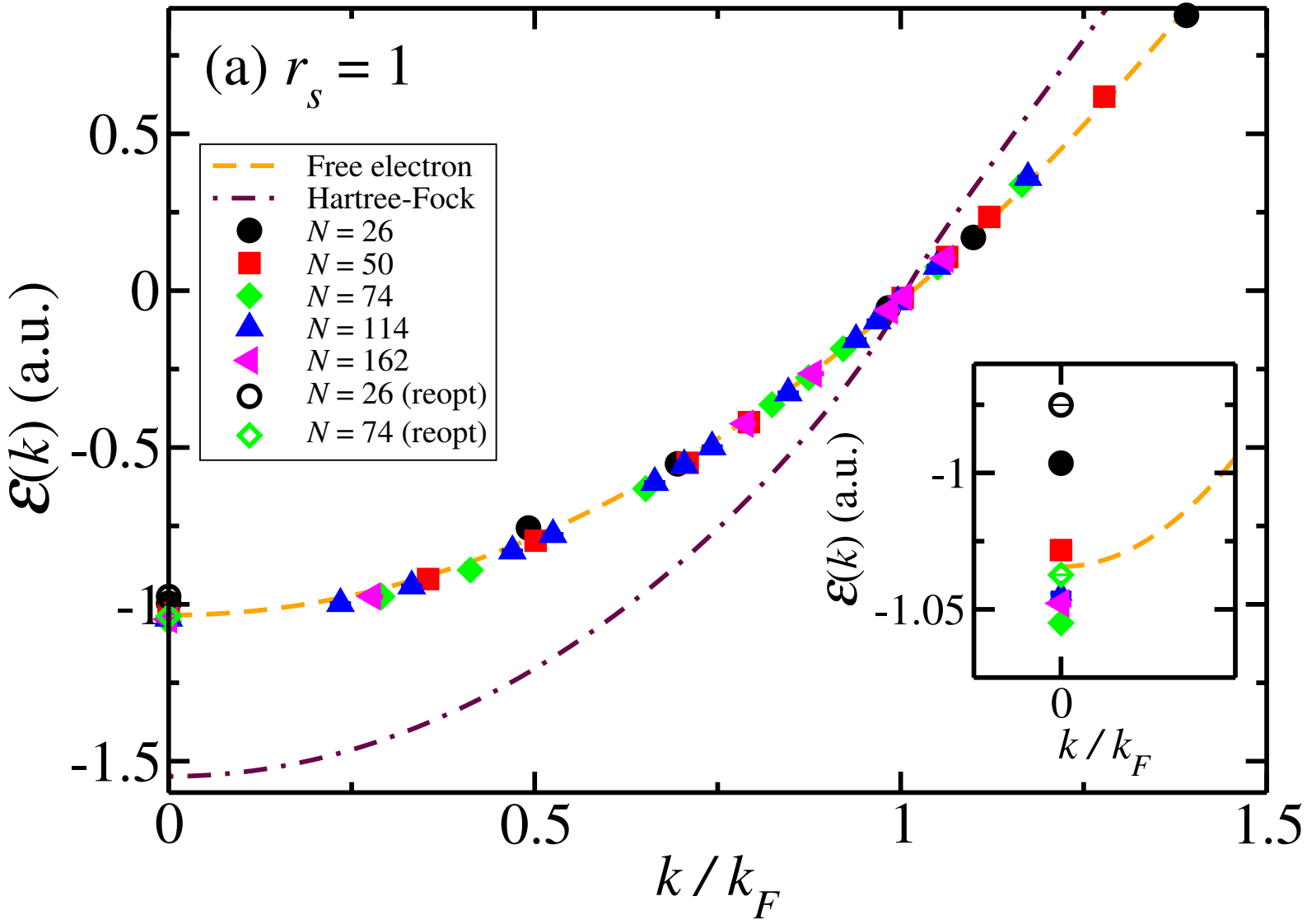

Paramagnetic Single-Particle Energy Band: $r_s = 5$

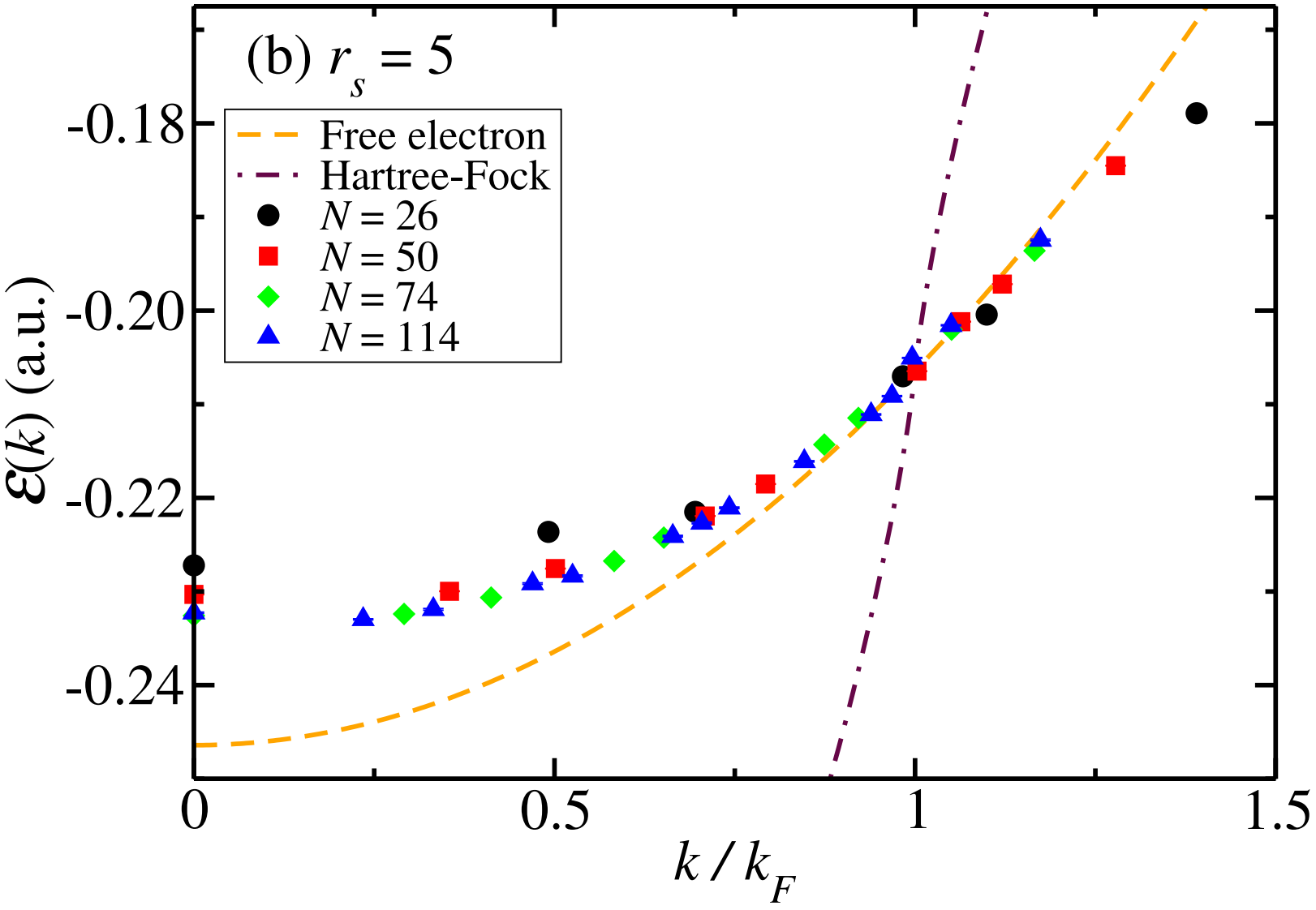

Paramagnetic Single-Particle Energy Band: $r_s = 10$

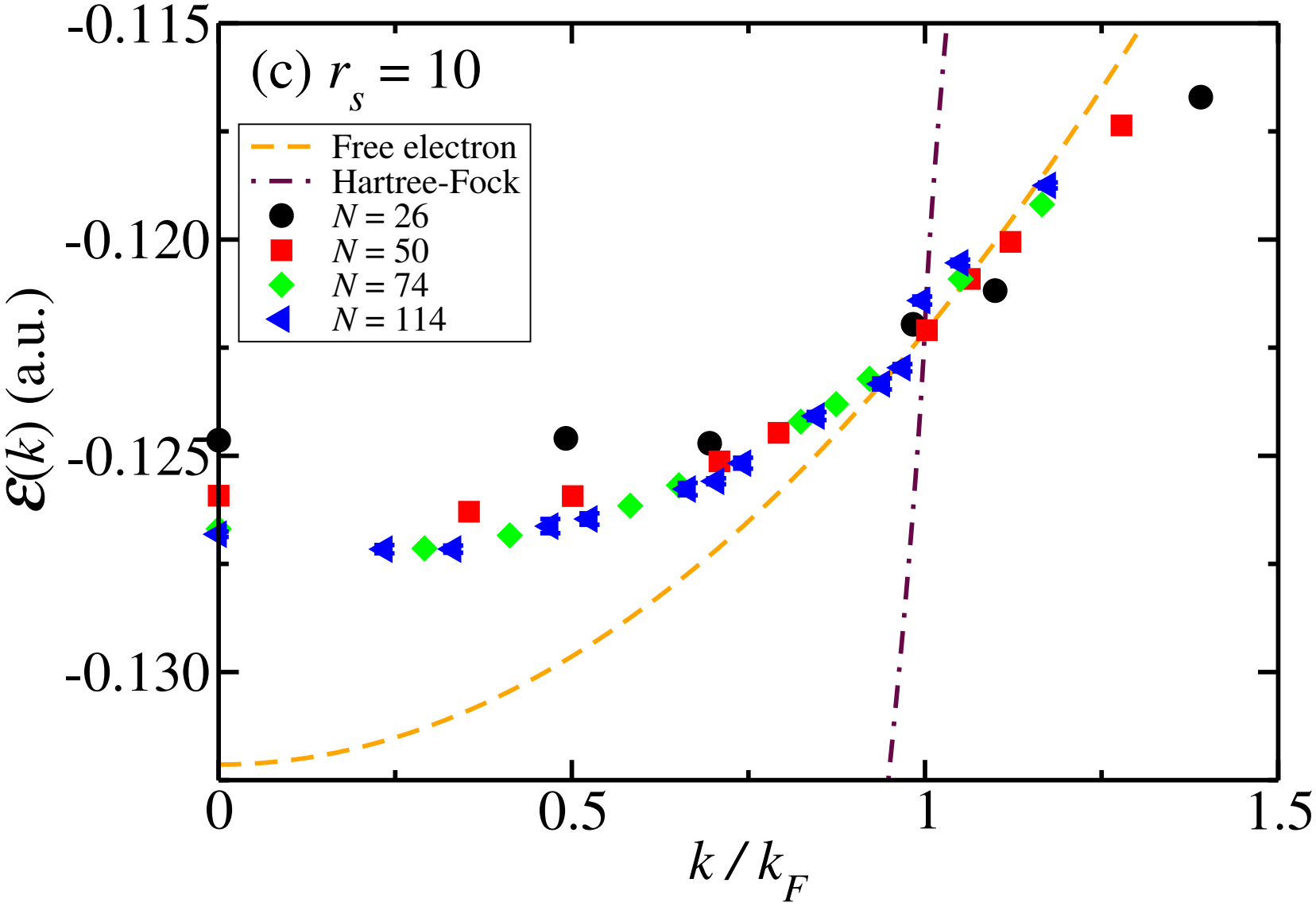

Ferromagnetic Single-Particle Energy Band: $r_s = 1$

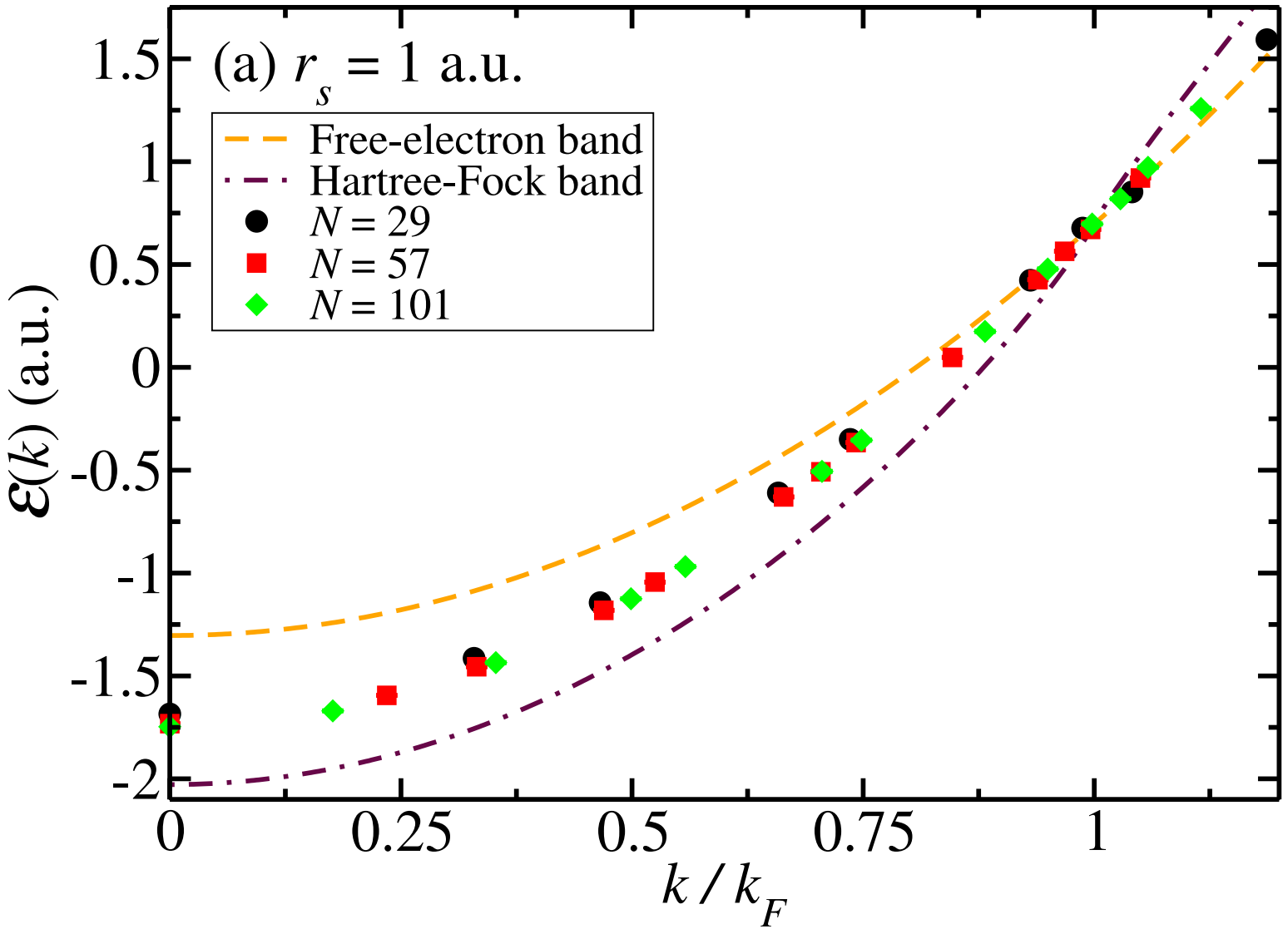

Ferromagnetic Single-Particle Energy Band: $r_s = 5$

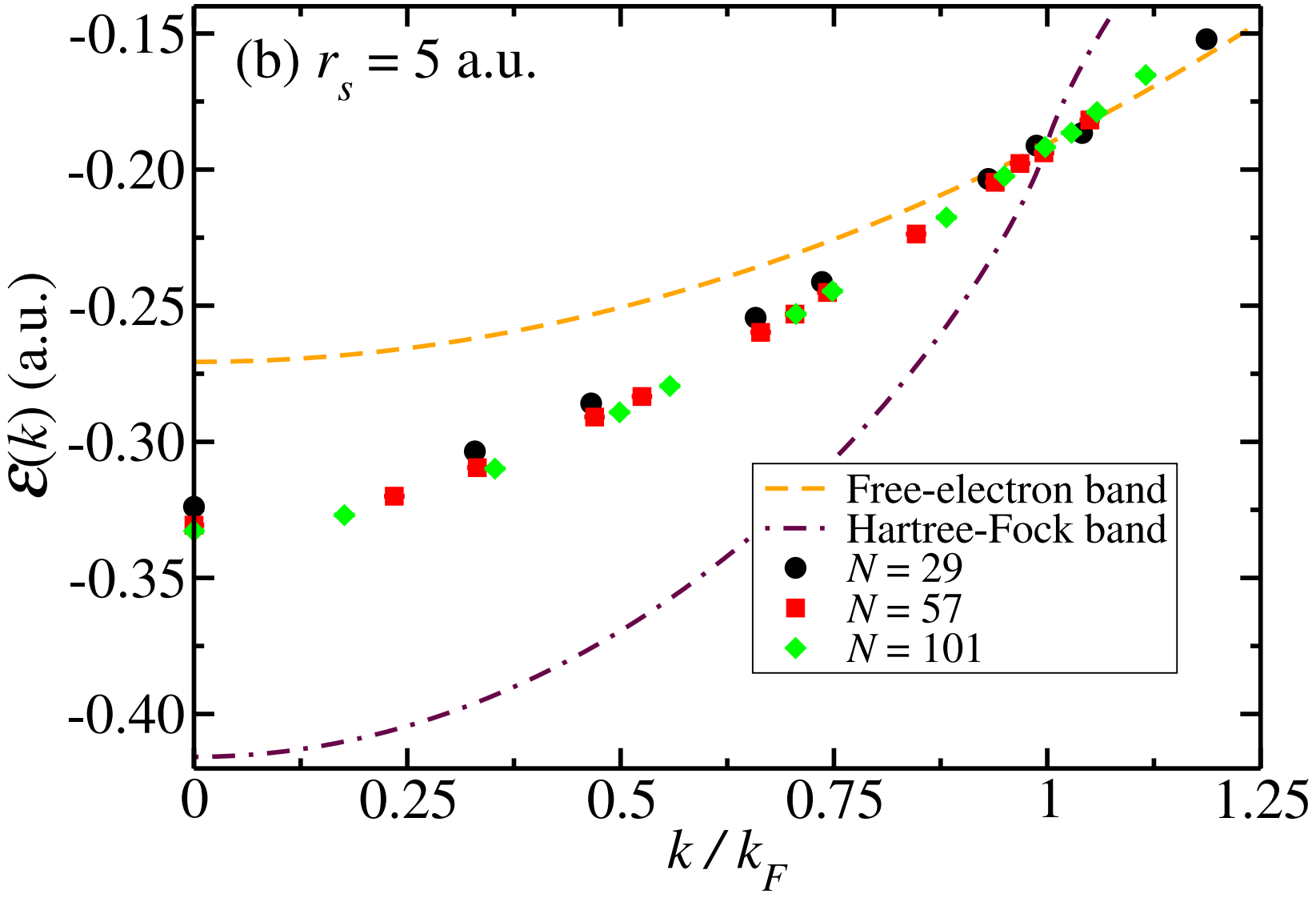

Ferromagnetic Single-Particle Energy Band: $r_s = 10$

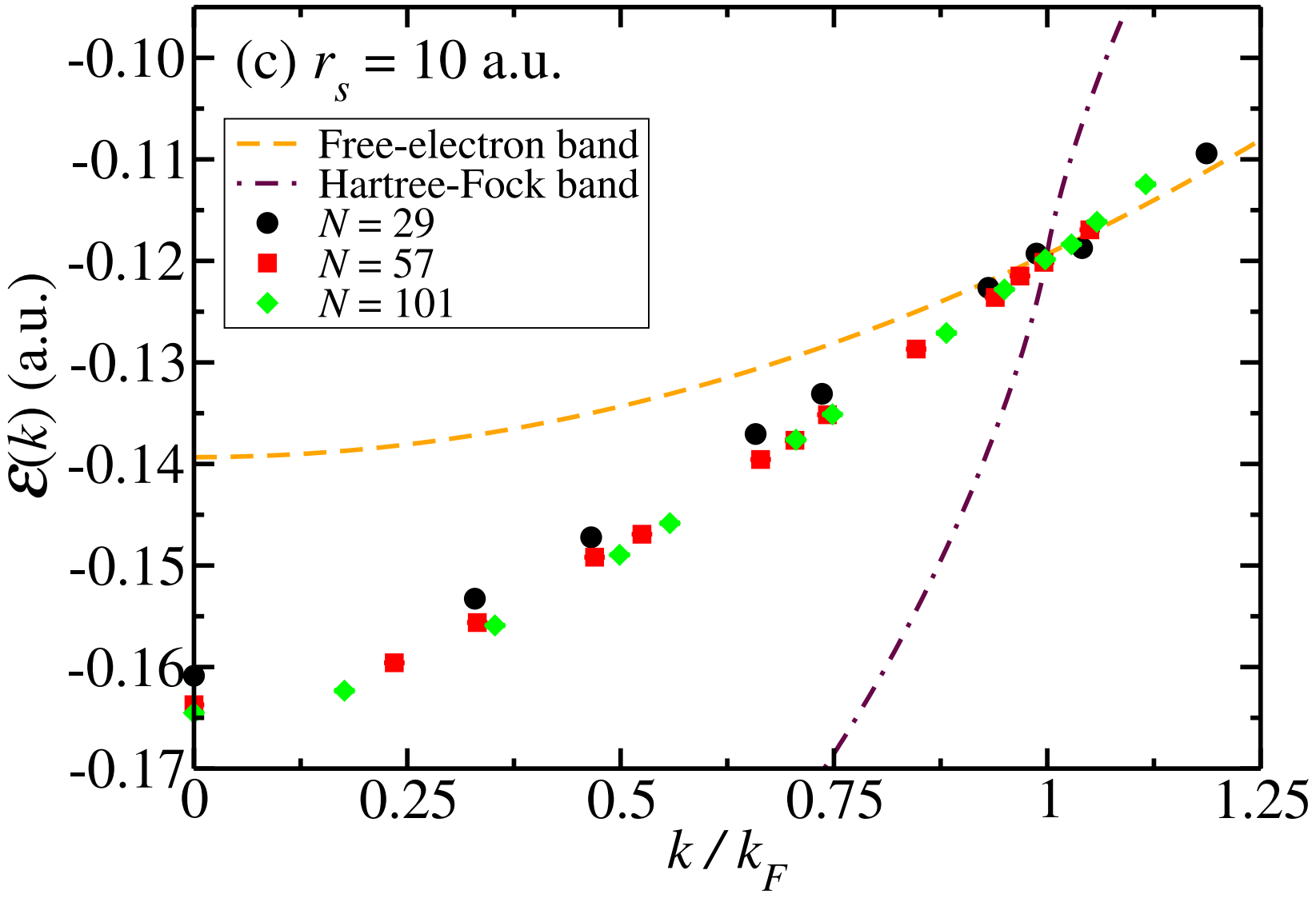

Extrapolation of the Effective Mass to the Thermodynamic Limit

- Effective mass against system size:

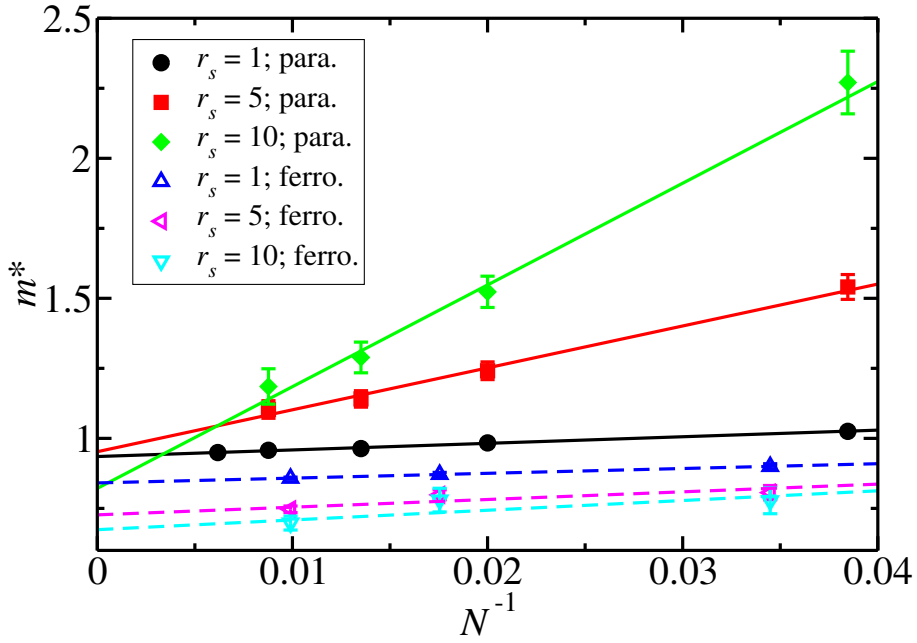

- Scaling is not the $N^{-1/4}$ predicted by Holzmann *et al.* near the Fermi surface, because we have fitted to the entire band.
  - Assume an N^{-1} scaling of the finite-size error.

Quasiparticle Effective Masses (I)

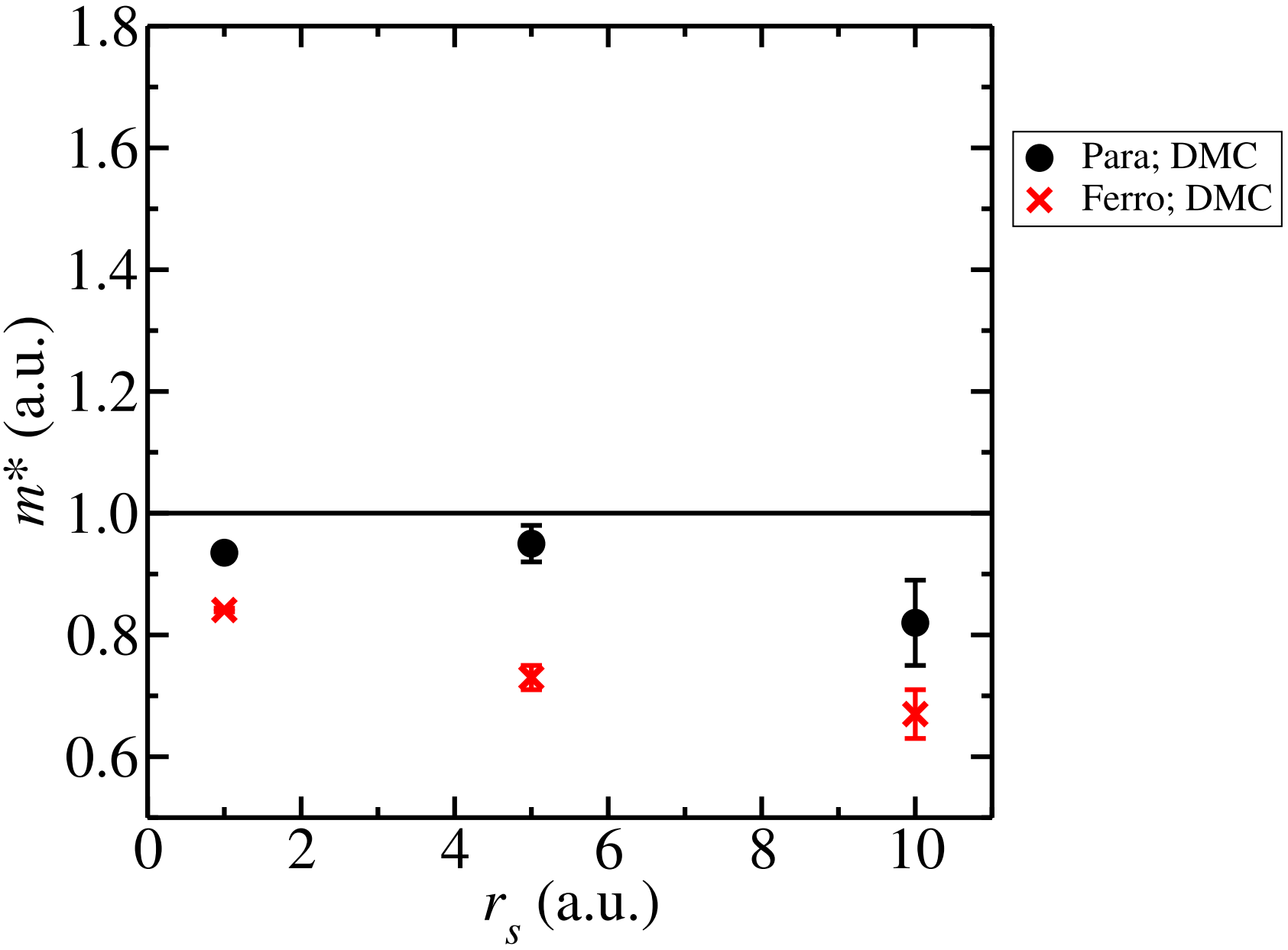

,

Quasiparticle Effective Masses (I)

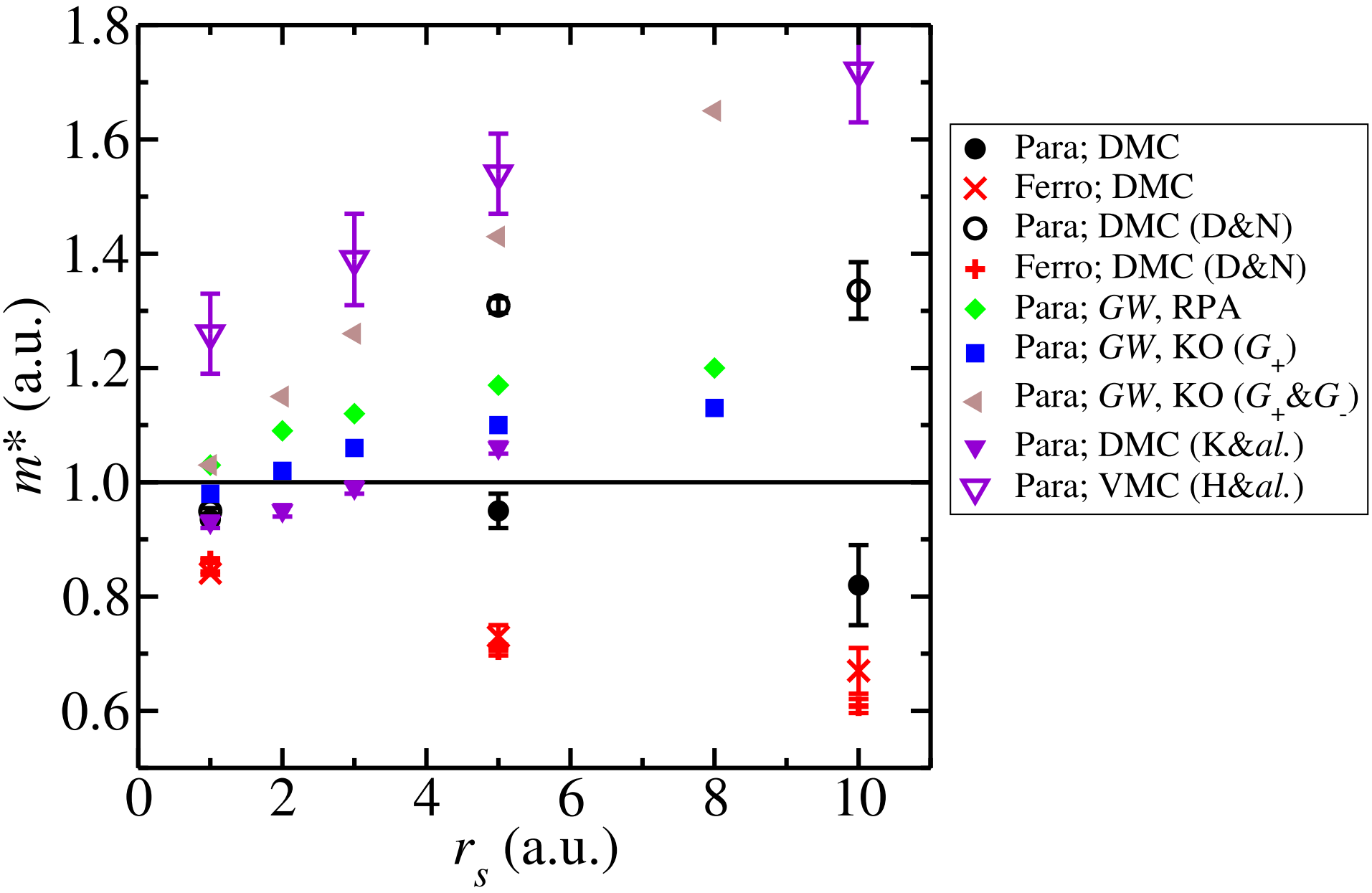

Quasiparticle Effective Masses (I)

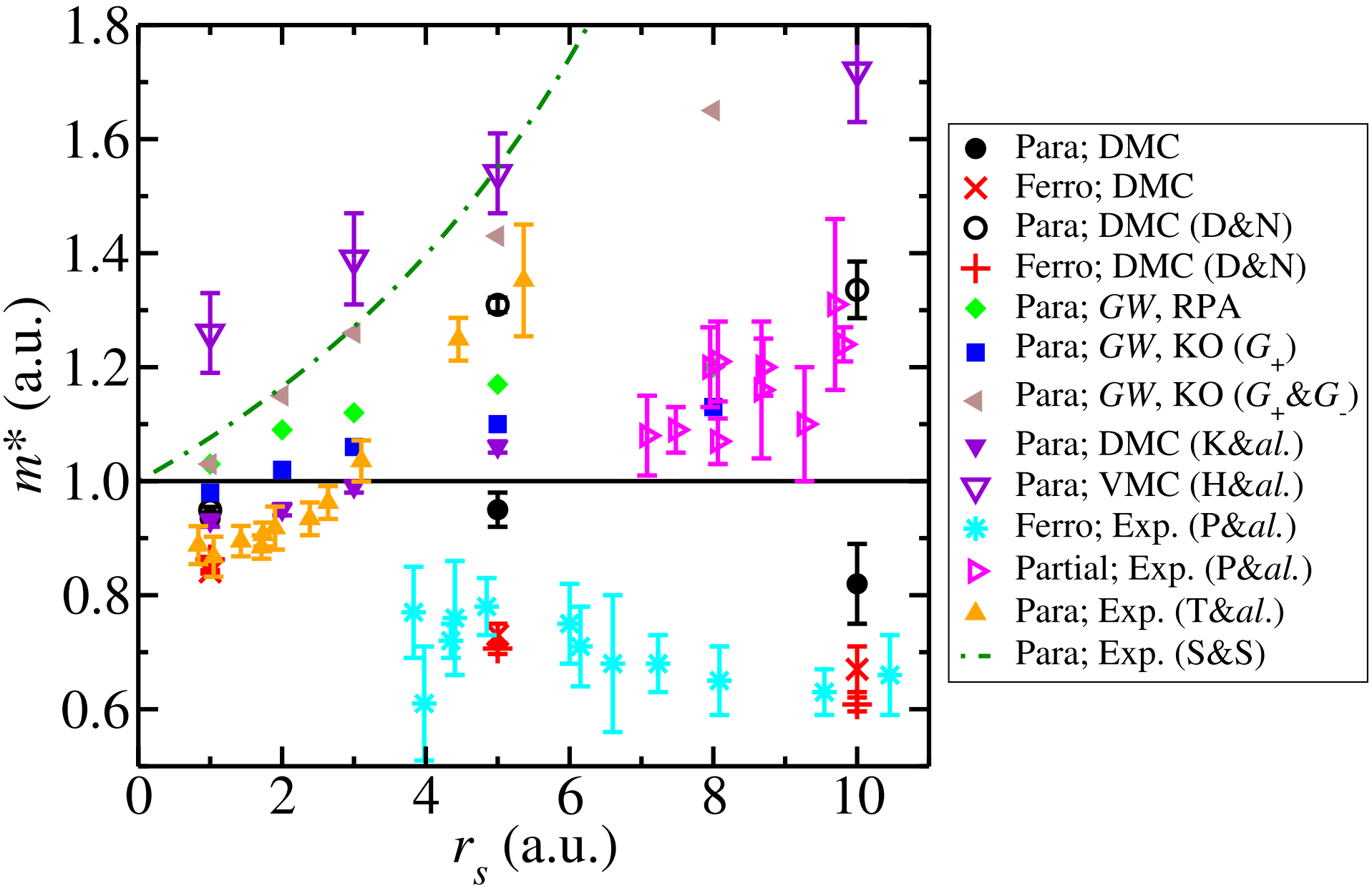

Quasiparticle Effective Masses (II)

- Paramagnetic HEG: effective mass remains close to 1.
- Ferromagnetic HEG: m^* *decreases* when the density is lowered.
- Our results therefore support the qualitative conclusions of Padmanabhan *et al.*
- Our results suggest that m^* in paramagnetic 2D HEGs does not grow rapidly as the density is reduced.

Conclusions

- *There is no region of stability for a ferromagnetic Fermi fluid in 2D.*
- *Wigner crystallisation occurs at $r_s = 31(1)$ a.u. in 2D. Crystallisation transition is from a paramagnetic fluid to a (frustrated) antiferromagnetic triangular crystal.*
- *Transition from an antiferromagnetic to a ferromagnetic crystal at $r_s = 38(5)$ a.u.*
- QMC results for contact PCF change little when wave function is improved. Suggests they are accurate. Disagreement with recent ladder theory calculation; agreement with old ladder theory calculation.
- Our data show that the quasiparticle effective mass of the ferromagnetic HEG decreases at low density, unlike the paramagnetic HEG.